

Lattice dynamics of lutetium

J. Pleschiutschnig and O. Blaschko

Institut für Experimentalphysik, Universität Wien, Strudlhofgasse 4, A-1090 Wien, Austria

W. Reichardt

Institut für Festkörperphysik, Kernforschungszentrum Karlsruhe, Postfach 3640, D-7500 Karlsruhe, Federal Republic of Germany

(Received 8 August 1989)

The normal-mode frequencies of lutetium were measured at 295 K by inelastic neutron scattering along the three main symmetry directions of the hexagonal lattice. The data are analyzed with a Born–von Kármán force model including interactions up to the eighth-nearest neighbors. The phonon-frequency-distribution function is calculated, and from that the lattice specific heat and the Debye temperature. The latter are found to be in good agreement with results from other experimental techniques.

I. INTRODUCTION

Our interest in the lattice dynamics of lutetium stems from recent investigations of hydrogen-ordering properties occurring in the rare-earth–hydrogen systems at lower temperatures.¹ In one of these works we studied the influence of hydrogen absorption on phonon properties of the hexagonal-closed-packed lutetium metal. Generally, hydrogen loading induces a frequency increase, as found by measurements essentially restricted to acoustic branches along two symmetry directions.

The lattice dynamics of the rare-earth metals holmium and terbium and that of the related scandium and yttrium

were studied by inelastic neutron scattering around 1970.^{2–6} Yet for lutetium, the most-heavy rare-earth element ($A_m = 175$), no complete set of dispersion relations was available until now. We therefore continued our investigation of the pure lutetium metal and are able to present the complete phonon dispersion relations in the three main symmetry directions. The measured frequencies were analyzed by a Born–von Kármán interatomic force model which reproduces the data quite well. We used the obtained set of force constants for calculating the inelastic structure factor and the phonon density of states. Finally, the lattice specific heat and the Debye temperature are evaluated and compared to experimental results found in the literature.

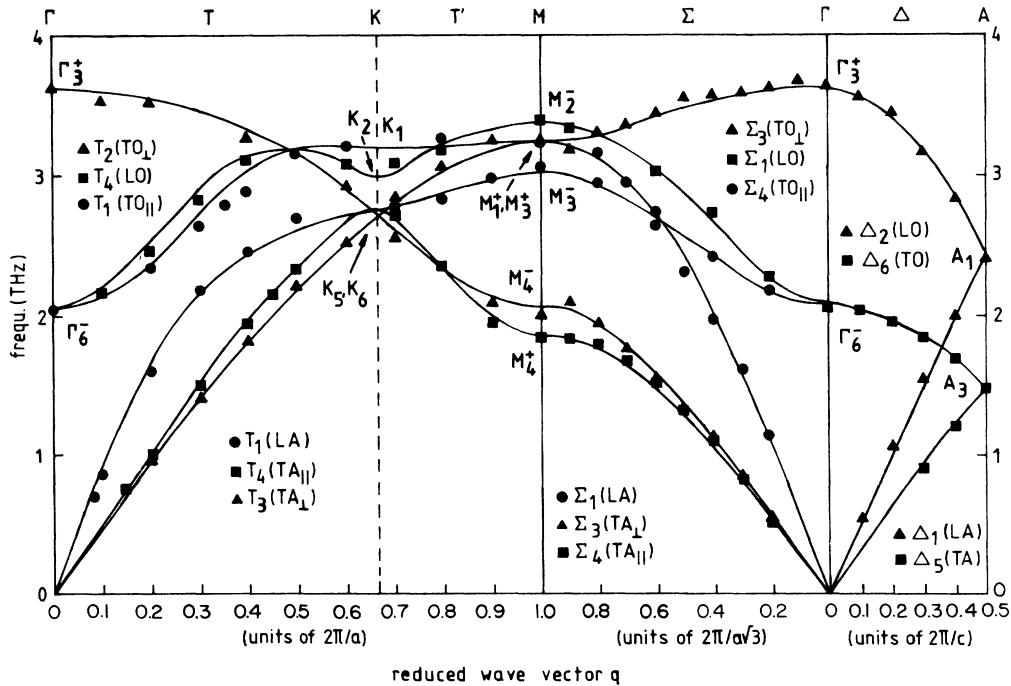


FIG. 1. Phonon dispersion curves for Lu at 295 K in the three main symmetry directions. The lines represent the results of an eighth-nearest-neighbor Born–von Kármán force model.

TABLE I. Measured phonon frequencies in Lu at 295 K, in THz.

q	$T_1(\text{LA})$	$T_1(\text{TO}_{\parallel})$	$T_2(\text{TO}_{\perp})$	$T_3(\text{TA}_{\perp})$	$T_4(\text{LO})$	$T_4(\text{TA}_{\parallel})$
$\Gamma-K-M$: q in units of $2\pi/a$						
0		2.04±0.01	3.63±0.02		2.04±0.01	
0.08	0.70±0.02					
0.1	0.86±0.02		3.54±0.01		2.16±0.02	
0.15						0.76±0.01
0.2	1.60±0.05	2.34±0.01	3.52±0.01	0.96±0.01	2.46±0.02	1.03±0.01
0.3	2.18±0.01	2.63±0.01		1.40±0.01	2.82±0.02	1.50±0.01
0.35		2.78±0.02				
0.4	2.45±0.01	2.88±0.05	3.26±0.02	1.82±0.02	3.10±0.01	1.94±0.01
0.45						2.15±0.01
0.5	2.69±0.01	3.14±0.01		2.21±0.02		2.34±0.02
0.6		3.20±0.02	2.92±0.01	2.52±0.02	3.08±0.01	
0.7	2.77±0.01		2.55±0.01	2.84±0.03	3.08±0.01	2.71±0.01
0.8	2.83±0.01	3.27±0.01		3.07±0.03	3.18±0.01	2.36±0.01
0.9	2.98±0.01		2.09±0.01	3.26±0.05		1.95±0.01
1.0	3.06±0.01	3.23±0.01	1.99±0.01	3.26±0.05	3.39±0.01	1.84±0.01
q	$\Delta_1(\text{LA})$	$\Delta_2(\text{LO})$	$\Delta_3(\text{TA})$	$\Delta_6(\text{TO})$		
$\Gamma-A$: q in units of $2\pi/c$						
0		3.63±0.02				2.04±0.01
0.1	0.55±0.01		3.57±0.01			2.02±0.02
0.2	1.05±0.01		3.45±0.01			1.95±0.01
0.3	1.54±0.01		3.17±0.01	1.90±0.01		1.84±0.01
0.4	2.00±0.01		2.83±0.01	1.20±0.01		1.68±0.01
0.5	2.41±0.01		2.41±0.01	1.47±0.01		1.47±0.01
q	$\Sigma_1(\text{LA})$	$\Sigma_1(\text{LO})$	$\Sigma_3(\text{TA}_{\perp})$	$\Sigma_3(\text{TO}_{\perp})$	$\Sigma_4(\text{TA}_{\parallel})$	$\Sigma_4(\text{TO}_{\parallel})$
$\Gamma-M$: q in units of $2\pi/a\sqrt{3}$						
0		2.04±0.01		3.63±0.02		2.04±0.01
0.1				3.67±0.01		
0.2	1.14±0.01	2.28±0.01	0.53±0.01	3.63±0.02	0.55±0.01	2.18±0.01
0.3	1.60±0.01		0.81±0.01	3.59±0.01	0.85±0.01	
0.4	1.96±0.01	2.72±0.01	1.12±0.01	3.57±0.02	1.09±0.01	2.41±0.01
0.5	2.31±0.01		1.32±0.01	3.55±0.01	1.31±0.01	
0.6	2.64±0.01	3.03±0.01	1.56±0.01	3.45±0.01	1.51±0.01	2.72±0.01
0.7	2.95±0.01		1.76±0.01	3.37±0.01	1.67±0.01	
0.8	3.16±0.01		1.95±0.01	3.31±0.01	1.79±0.02	2.94±0.01
0.9		3.33±0.01	2.10±0.01	3.18±0.01	1.83±0.01	
1.0	3.23±0.01	3.39±0.01	1.99±0.01	3.26±0.05	1.84±0.01	3.06±0.01

II. MEASUREMENTS AND RESULTS

The experiment was carried out on the triple-axis spectrometer 2T located at the thermal neutron source of the Orphée reactor from the Laboratoire Léon Brillouin in Saclay, France. The measurements were done with a fixed final energy $E_f = 14.7$ meV. A pyrolytic-graphite filter was mounted between the sample and the analyzer. We used a copper monochromator, Cu(111), and a pyrolytic-graphite analyzer, PG(002). The collimations were 50'-30'-49'-49', starting with the in-pile collimator. Some phonon groups which suffered from unfavorable structure factors were measured with a focusing monochromator and analyzer. The scans were run in the constant- Q mode, with the exception of some acoustic phonons in the vicinity of the Γ point, which we mea-

sured by constant-energy scans.

The lutetium single crystal was grown by D. A. Hukin, Clarendon Laboratory, Oxford; its volume was 0.5 cm³. The 99.9% sublimed-grade ingot delivered by Rare Earth Products, Ltd., Great Britain, had been zone-refined by cold-crucible induction heating. The principal gaseous impurity were several tenths of an at. % of oxygen. The mosaic spread was 0.5°. Some measurements were also undertaken after two hydrogen-loading and -degassing procedures, which increased the spread by a factor 2.

In Table I we list the results for the three principal directions $\Gamma-K-M$, $\Gamma-M$, and $\Gamma-A$, and in Fig. 1 the dispersion curves are plotted. They look similar to those found for terbium² and holmium.^{3,4} The experimentally determined slopes of acoustic modes governed by the same elastic constant differ within a few percent. A com-

TABLE II. Comparison of ultrasound velocities in km/s as gotten from the initial slopes of the acoustic modes with direct measurements from Greiner *et al.* (Ref. 7) (GBS).

Veloc.	Direc.	This work	GBS	Δ (%)
v_{11}	$[\xi\xi 0]$	3.014	2.993	0.7
v_{11}	$[\xi 00]$	3.127	2.993	4.3
v_{33}	$[00\xi]$	2.897	2.895	0.1
v_{44}	$[\xi\xi 0]$	1.647	1.660	-0.8
v_{44}	$[\xi 00]$	1.630	1.660	-1.8
v_{44}	$[00\xi]$	1.665	1.660	0.3
v_{66}	$[\xi\xi 0]$	1.647	1.670	-1.4
v_{66}	$[\xi 00]$	1.630	1.670	-2.4

parison with ultrasound data from Greiner *et al.*⁷ gives deviations of the same order of magnitude (Table II).

III. MODEL CALCULATIONS

A. Born-von Kármán fit

The data were analyzed by means of a least-squares-fit procedure within the frame of a Born-von Kármán force model. The computer program is based on the axially symmetric model (AS model) proposed by Lehman *et al.*,⁸ which requires only two independent parameters per shell. A first attempt taking into account interactions up to the eighth-nearest neighbors brought about satisfying results, with the exception of the lower T_1 (LA) branch around the K point. The AS model predicts a degenerate mode for this and the upper T_4 (LO) branch at the K point, contrary to the observed degeneracy of the two lower T_1 and T_4 branches. For terbium Houmann and Nicklow² used a mixed force model which gives quite good results. They start with general interactions (tensor forces) up to the fourth-nearest neighbors and continue with axially symmetric ones to the eighth next-nearest neighbors.

In the case of the general-tensor-force model (GTF model), zone-boundary data are necessary to determine the off-diagonal elements of the dynamical matrices for the first- and the third-neighbor interaction since they do not enter in the dispersion relations for the three main symmetry directions. If one carries out calculations restricted to these three directions, the two force-constant models differ only in the matrix for the second neighbors within the first four shells. Besides the common diagonal elements, the GTF matrix consists of an asymmetric off-diagonal one, $\alpha_{12} = -\alpha_{21}$. As we did not perform measurements along the zone boundaries, we took advantage of the described relation between the two force-constant models in the restricted case and made a second approach with a slightly modified AS model. For the second-nearest-neighbor interaction the dynamical matrix is enlarged by an asymmetric off-diagonal element normally absent in an AS model. This additional force constant is not concerned by the procedure of variation of the ordinary AS parameters. Its numerical value was

TABLE III. Force constants for lutetium obtained by a least-mean-squares fit and an eighth-nearest-neighbor, axially symmetric interaction model. $\alpha_k^n = (x_i^n x_k^n / r^2)(F_n - G_n) + G_n \delta_{ik}$, $r^2 = [(x_i^n)^2 + (x_j^n)^2 + (x_k^n)^2]$, $n = 1, 2, \dots, 8$.

Neighbor n	Typical coord.	Pair of force constants (F_n, G_n) (dyn/cm)
1	$(0, a/\sqrt{3}, c/2)$	(19 968, 1177)
2	$(a, 0, 0)$	(15 378, 347, 2200 ^a)
3	$(0, 2a/\sqrt{3}, c/2)$	(-2839, -614)
4	$(0, 0, c)$	(-4141, -1615)
5	$(a/2, 5a/2\sqrt{3}, c/2)$	(1508, -176)
6	$(0, a\sqrt{3}, 0)$	(1688, 83)
7	$(a, 0, c)$	(394, 281)
8	$(2a, 0, 0)$	(-306, -71)

^aAdditional force constant (see text).

chosen after the results for Tb (Ref. 2) and Ho (Ref. 4), just as our initial set of the other 16 parameters. With this modification for the second-neighbor shell of the AS model, we reached a quite sufficient agreement between the calculated and measured eigenfrequencies. In Table III the values for the force constants are listed.

From this set of force constants we calculated the inelastic structure factor

$$g_j^2(\mathbf{q}, \tau) = \frac{b^2}{m v_j(\mathbf{q})} \left| \sum_s \mathbf{e}_{sj} \cdot \mathbf{Q} \exp(i\tau \cdot \mathbf{r}_s) \right|^2$$

with \mathbf{q} the phonon wave number, τ a reciprocal-lattice point, \mathbf{Q} the scattering vector, b the coherent-scattering length, m the atomic mass, and \mathbf{e}_{sj} the eigenvector of the s th atom at position \mathbf{r}_s in the unit cell vibrating in the j th mode, for a variety of τ points and the three main symmetric directions. In general, mixing of modes belonging to the same symmetry group is the rule, as was already demonstrated for other hcp structures in the literature, e.g., Ref. 2.

B. Phonon density of states, lattice specific heat, and Debye temperature

The final set of force constants was used to calculate the frequency distribution function $g(\nu)$ (Fig. 2). The

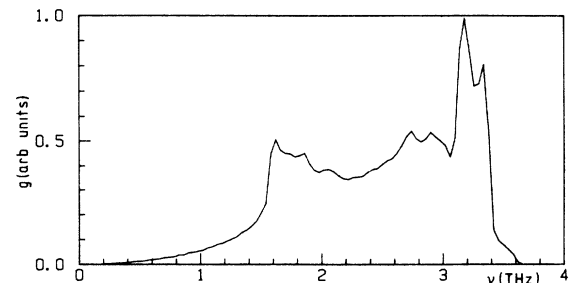


FIG. 2. Calculated phonon-frequency-distribution function $g(\nu)$ for Lu (unsmoothed computer plot).

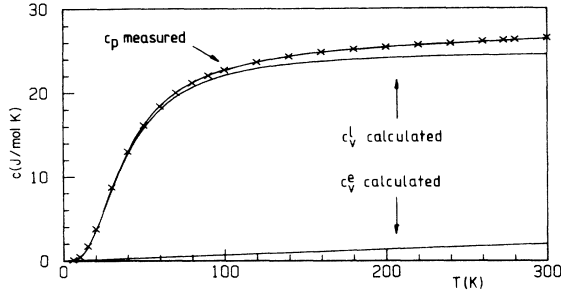


FIG. 3. Lattice specific heat for lutetium calculated from the phonon density of states. The experimental values of the heat capacity found by Gerstein *et al.* (Ref. 9) and the result of the measurement of the electronic specific heat of Lu of Wells *et al.* (Ref. 10) also are shown.

calculation followed the root-sampling method, dividing the irreducible section of the first Brillouin zone into a mesh of 17 391 points. The width of the histograms, $g(\nu)\Delta\nu$, in the plot is 0.04 THz. The phonon density of states is quite similar to those gotten for terbium and holmium.^{2,4}

From the frequency distribution, the lattice specific heat c_v^l as a function of temperature at constant volume was calculated. The result is shown in Fig. 3, where one also finds the values for c_p of Gerstein *et al.*⁹ from calorimetric methods. If the electronic contribution $c_v^e = \gamma T$ with $\gamma = 6.8 \text{ mJ K}^{-2} \text{ mol}^{-1}$ taken from Ref. 10 is added, the data are in good agreement.

Finally, we computed the Debye temperature Θ as a function of temperature from our results for the lattice specific heat (Fig. 4). For $T=0$ we find $\Theta(0) = 188 \text{ K}$, and $\Theta = 159 \text{ K}$ in the high-temperature limit. The curve has a minimum of 155.8 K at 23 K. For comparison, recent data on the Debye temperature from lutetium obtained by x-ray measurements indicate $\Theta = 157 \pm 1 \text{ K}$.¹¹ In the zero-temperature limit Tonnie's *et al.*¹² derive, from measurements of the elastic constants, $\Theta(0) = 184.5 \text{ K}$. If one is reminded that our value is based on the phonon density of states at 295 K and no correction due to anharmonicity was made, the difference of 2% is reasonable.

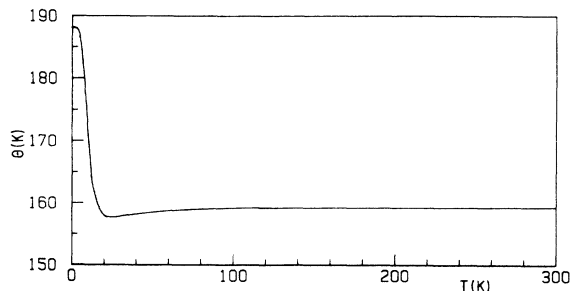


FIG. 4. Debye temperature as a function of temperature for Lu determined from the calculated lattice specific heat.

IV. DISCUSSION AND CONCLUSION

The measured phonon frequencies of lutetium and the results derived therefrom are close to those found in terbium and holmium (see Table IV). However, a trend to higher frequencies with increasing atomic weight is visible, which is in contradiction to a scaling of the frequencies with the inverse of the square root of the atomic mass. Therefore the interatomic forces in the three metals differ to a nonnegligible extent, despite the similarity of their dispersion curves. The reason for this lies presumably in the electronic structure, which is supported by the fact that the coefficients γ for the electronic specific heat in Tb and Lu are different.¹⁰ A closer inspection gives $\nu_{\text{Lu}}^2/\nu_{\text{Tb}}^2 = 1.25$ on the average. With $m_{\text{Lu}}/m_{\text{Tb}} = 1.10$ we obtain 1.38 as scaling factor for the force constants of the two metals.

The misfit of the AS model for the lower T_1 (LA) branch around the K point is of inherent character. In the case of hexagonal lattices the classification of the normal modes by the irreducible representations of the space groups for the high-symmetry directions and points yields two doubly degenerate modes ν_5 and ν_6 at K , adopting the notation of Raubenheimer and Gilat.¹³ The latter mode is compatible to the T_2 and T_3 branches, whereas the compatibility relation for ν_5 is less stringent. It belongs to one of the T_1 and T_4 branches. Now the AS and every other central-force model demand at the K point $\nu_1^2 + \nu_2^2 = 2\nu_5^2$.¹⁴ With $\nu_1(\text{TO}_{\parallel})$ the highest frequency in Lu at K (Fig. 1), the AS model gives $\nu_1 > \nu_5 > \nu_2$ in order to save the sum rule, thus placing the doubly degenerate mode in between. The actually observed arrangement of the frequencies is $\nu_1 > \nu_2 > \nu_5$, which violates the restriction of axial symmetry. Therefore, in principle, only a more complex force model is able to describe the real situation.

On the other hand, the stated sole difference in the dynamical matrices of the two models for the three main symmetry directions and the good results gotten with the AS model, apart from the singular failure at the K point, led us to the assumption that a slight modification concerning the second-neighbor interaction only would be sufficient to break the restriction of axial symmetry at K . In fact, the addition of a second matrix with only two asymmetric xy elements different from zero to the ordinary AS matrix for the second-neighbor interaction brought the desired result. For simple economical reasons the additional parameter does not enter the fit procedure.

Strictly speaking, we make use of a "mixed" force model with tensor forces for the second neighbors and axially symmetric forces for the others on the mathematical basis of the AS model. Further justifications for our procedure, besides the good quality of the data fit, are the strong similarity of the frequency distribution obtained with those of the related elements Tb and Ho calculated on the basis of a mixed force model as cited, and the agreement between the calculated and measured values of the derived properties specific heat and Debye temperature.

TABLE IV. Selected normal-mode frequencies in Tb, Ho, and Lu, in THz. The values for Tb and Ho stem from Refs. 2 and 4.

	Γ_6^-	Γ_3^+	A_3	A_1	M_4^-	M_4^+	M_3^+	M_2^-	M_1^+
Tb	1.82	3.25	1.30	2.44	1.75	1.59	2.90	3.05	2.89
Ho	1.94	3.40	1.34	2.56	1.96	1.65	3.04	3.08	3.05
Lu	2.04	3.63	1.47	2.41	1.99	1.84	3.26	3.39	3.23

ACKNOWLEDGMENTS

This work was partly supported by the Fonds zur Förderung der wissenschaftlichen Forschung, Austria.

The Laboratoire Léon Brillouin (Saclay), where the experiments were carried out, is a joint research institute of the Centre National de la Recherche Scientifique and the Commissariat à l'Énergie Atomique.

-
- ¹O. Blaschko, G. Krexner, J. N. Daou, and P. Vajda, *Phys. Rev. Lett.* **55**, 2876 (1985); O. Blaschko, G. Krexner, L. Pintschovius, P. Vajda, and J. N. Daou, *Phys. Rev. B* **38**, 9612 (1988); O. Blaschko, G. Krexner, J. Pleschiutchnig, G. Ernst, J. N. Daou, and P. Vajda, *ibid.* **39**, 5605 (1989).
- ²J. C. Gylden Houmann and R. M. Nicklow, *Phys. Rev. B* **1**, 3943 (1970).
- ³J. A. Leake, V. J. Minkiewicz, and G. Shirane, *Solid State Commun.* **7**, 535 (1969).
- ⁴R. M. Nicklow, N. Wakabayashi, and P. R. Vijayaraghavan, *Phys. Rev. B* **3**, 1229 (1971).
- ⁵S. K. Sinha, T. O. Brun, L. D. Muhlestein, and J. Sakurai, *Phys. Rev. B* **1**, 2430 (1970).
- ⁶N. Wakabayashi, S. K. Sinha, and F. H. Spedding, *Phys. Rev. B* **4**, 2398 (1971).
- ⁷J. D. Greiner, B. J. Beaudry, and J. F. Smith, *J. Appl. Phys.* **62**, 1220 (1987).
- ⁸G. W. Lehman, T. Wolfram, and R. E. De Wames, *Phys. Rev.* **128**, 1593 (1962).
- ⁹B. C. Gerstein, W. A. Taylor, W. D. Shickell, and F. H. Spedding, *J. Chem. Phys.* **51**, 2924 (1969).
- ¹⁰P. Wells, P. C. Lanchester, D. W. Jones, and R. G. Jordan, *J. Phys. F* **6**, 11 (1976).
- ¹¹T. H. Metzger, P. Vajda, and J. N. Daou, *Z. Phys. Chem. (Neue Folge)* **143**, 129 (1985).
- ¹²J. J. Tonnie, K. A. Gschneidner, Jr., and F. H. Spedding, *J. Appl. Phys.* **42**, 3275 (1971).
- ¹³L. J. Raubenheimer and G. Gilat, *Phys. Rev.* **157**, 586 (1967).
- ¹⁴J. L. Warren, *Rev. Mod. Phys.* **40**, 38 (1968).